Vol. 67: 257–269, 2016
doi: 10.3354/cr01361

CLIMATE RESEARCH
Clim Res

Published March 14

Precipitation change between 1960 and 2006 in the Qiantang River basin, eastern China

Fang Xia[1], Xingmei Liu[1,*], Jianming Xu[1], Lejiang Yu[2], Zhou Shi[1]

[1]College of Environmental and Natural Resource Sciences, Zhejiang University, Hangzhou 310058, PR China
[2]Applied Hydrometeorological Research Institute, Nanjing University of Information Science & Technology, Nanjing 211167, PR China

ABSTRACT: Precipitation in a typical basin of the Qiantang River, which is a vital component of the freshwater supply of Zhejiang province, eastern China, was analyzed for spatial and temporal changes from 1960–2006, based on daily precipitation measured at 14 meteorological stations. Although regional annual precipitation did not reveal any significant trends, distinct inter-decadal variation was identified when an integrated precipitation indicator was applied. Trends in annual precipitation with different magnitudes and their corresponding frequencies were characterized by different spatial distribution patterns. Analysis of extreme precipitation events indicated more extreme precipitation after the mid-1980s, which is consistent with the results of a dry/wet condition analysis. Both the significant increase in summer precipitation and the transition from a consecutive dry period to a relatively wet period after the mid-1970s suggest that this region is becoming wetter and may be prone to more floods during the summer. The variation in summer precipitation was largely captured by an empirical orthogonal functions (EOF) analysis, and the similar variation in the first principal component proved the applicability and effectiveness of the EOF analysis. Regional factors, such as aerosols, land reclamation and the extent of irrigation, combined with large scale circulation may have influenced the observed change in precipitation. This research provides insight into historical change in precipitation, and will aid in future disaster forecasting/warning.

KEY WORDS: Extreme precipitation · Summer precipitation · Spatio-temporal variation

Resale or republication not permitted without written consent of the publisher

1. INTRODUCTION

Climate change, especially changes in precipitation, has received increasing attention worldwide in recent decades. Precipitation is among the most important components of climate and hydrological systems. Enhanced changes in precipitation, which have been primarily attributed to global warming, have a significant effect on water resources, such as the frequency, intensity, and duration of droughts and floods, and can cause tremendous financial costs and loss of human life (Piao et al. 2010, Bouwer 2011). Changes in precipitation affect ecosystem processes, especially plant growth and ecosystem carbon balance (Wu et al. 2011). Furthermore, extreme precipitation, including floods and droughts, can increase the vulnerability of ecosystems (Yu et al. 2012). The Intergovernmental Panel on Climate Change (IPCC) reported an increase in global average precipitation, and also indicated a decrease in the precipitation amount at subtropical latitudes and a significant increase at the northern high latitudes (IPCC 2013). Model projections have also been employed to understand historical changes in precipitation, as well as future changes (Bukovsky & Karoly 2011, Chen & Frauenfeld 2014).

Despite previous studies of global warming impacts on precipitation, there is still a need to evaluate precipitation changes at regional and watershed levels, due to the different local environmental con-

*Corresponding author: xmliu@zju.edu.cn

© Inter-Research 2016 · www.int-res.com

ditions which can influence the local precipitation variation to a certain extent. Historical large-scale precipitation observations and forecasts are less helpful in local-scale planning, because precipitation changes, especially changes in extreme events, vary among regions. Precipitation changes do not appear simultaneously and uniformly, and they exhibit a strong correlation with the local climate and other regional factors such as geographical variation and local sources of aerosols. Although an individual extreme precipitation event is usually insignificant on a large scale due to its specific scope of influence and duration, it may be fatal on a sub-regional scale. The IPCC confirmed the substantial variation in precipitation among regions in the 21st century (IPCC 2014). Various studies have investigated regional precipitation changes. Chaplot (2007) employed a Soil and Water Assessment Tool model to predict the response of water and soil resources to global climate change, and emphasized the importance of watershed-level investigations. Applying multivariate methods, Dinpashoh et al. (2004) divided the precipitation climate of Iran into 7 regions, and the results showed different types of growth curves. An investigation into Krakow, Poland, was performed to identify the long-term variability of different types of regional precipitation in winter and demonstrate the influence of regional air temperature on the changes in winter precipitation (Twardosz et al. 2012). A regional difference was also identified across the US by Portmann et al. (2009), which also confirmed the existence of a 'warming hole' (Kunkel et al. 2003). Studies of spatial variation in precipitation have also been conducted in China (Yuan et al. 2010, Zhang et al. 2011). For example, You et al. (2011) concluded that the frequency and intensity of precipitation in China varied among regions, and were mostly influenced by the summer monsoon and Mongolia geopotential height, which redistributed the water vapor flux in the atmosphere.

Recent studies have proven a widening range in precipitation between wet and dry seasons, which may cause frequent droughts and floods (Chou et al. 2013). Summer precipitation in China is primarily dominated by the East Asia summer monsoon and several other factors. An abrupt change in summer climate (temperature and rainfall) was recorded around the mid-1970s in East Asia and was related to the intensification and westward and southward extension of the western Pacific subtropical high, the variations of geopotential height over Eurasia, and the change in sea surface temperature over the tropical Indian Ocean and tropical western Pacific (Hu 1997). Similar findings were also reported by Wang (2001). Numerous studies have investigated the patterns of change in summer precipitation in China. For example, analyzing the summer precipitation from 1957–2008 revealed a 'north drying and south wetting' pattern in China (Ye et al. 2013). Zhai et al. (2005) recorded inter-decadal variation in summer precipitation in eastern China, which substantially correlated with the Asian summer monsoon. Compared to the period from 1979–1990, the Huang-Huai River region showed increased summer precipitation, whereas summer precipitation decreased in the Yangtze River region from 2000–2008 (Zhu et al. 2011).

The Qiantang River basin is located in eastern China, which is characterized by rapid economic development, an explosion in population, and high levels of urbanization. The Qiantang River provides fresh water to Zhejiang province. However, this region has experienced droughts and floods in recent decades, which resulted in significant economic costs and losses of human life (Dai et al. 1998). Such costs are extremely severe during the typhoon seasons, when typhoons produce extreme heavy precipitation. In 2011, a serious flood that occurred in this region due to continuous heavy rainfall events was considered to be the largest flood since the 1950s. Several projections have been carried out for this region to investigate changes in precipitation in the 21st century. By applying weather generator downscaling, simulations of extreme precipitation in the 21st century have been developed, and the study region has shown an increasing trend of extreme precipitation events in various general circulation models and emission scenarios (Xu et al. 2012). Precipitation will increase over high elevation areas in this region, while decreases in precipitation will occur over the plains in the late 21st century (Xu et al. 2014). However, there are few detailed studies about historical precipitation, especially with respect to changes in precipitation of different magnitudes and at multiple scales. Understanding historical climate characteristics, which significantly affect the hydrological cycle, is critical for improving water management and disaster warning.

This study primarily focused on the changes in precipitation from 1960–2006 in this region. We selected this period to be consistent with the temperature analysis in our previous study (Xia et al. 2015). Here we examined daily precipitation series to achieve the following objectives: (1) detect possible trends in annual and summer precipitation, as well as extreme precipitation events, (2) identify spatio-temporal

variation in annual and summer precipitation for the long-term series, and (3) identify the main modes of summer precipitation variation.

2. MATERIALS AND METHODS

2.1. Study region and meteorological data

The Qiantang River basin, which is among the most economically developed regions in eastern China, is mainly located in Zhejiang Province. This region is divided into 3 sub-catchments: Lanjiang, Xin'anjiang, and Fuchunjiang. The total drainage is approximately 55 600 km^2, with a main stream length of 688 km. This region is primarily dominated by the sub-tropical monsoon climate, with an annual average temperature of ~17°C, and an annual average precipitation of ~1600 mm. In addition to the monsoon climate, this region has varied topography, which produces heterogeneous precipitation over the basin. The summer is characterized by high temperatures and abundant precipitation, whereas the winter is cold and dry. Monthly precipitation is distributed with a bimodal pattern in a year, in which the first rainy season begins in May and the second rainy season begins in August. During these 2 rainy seasons, which are always referred to as plum season and typhoon season, consecutive rainy days or heavy precipitation always occur (Tian et al. 2012).

To detect precipitation variation over the past decades, we selected daily precipitation data from 14 meteorological stations in this basin (Fig. 1); details about these meteorological stations were provided in our previous study (Xia et al. 2015). Various methods, including the cumulative deviations test (Buishand 1982), Bayesian procedures (Chernoff & Zacks 1964, Gardner 1969), the standard normal homogenization test (Alexandersson & Moberg 1997), and the Pettitt test (Pettitt 1979), were employed to detect non-homogeneity of the precipitation data, which may be caused by relocation, instrument changes, and other unnatural factors. These methods were executed in Anclim software (Štěpánek 2008). The results indicated that all stations in this study were homogeneous at a significance level of 0.05. Data quality control of the outliers and the missing data was conducted using Rclimdex software. A year with >1 mo of missing data or >1 wk of consecutive missing data was eliminated, and the gap was filled with the average of 3 neighboring stations for the same day, month, and year. If the data were missing for 1 or 2 d, the gap was filled with an average of the neighboring 4 d (2 d earlier and 2 d later). The monthly, seasonal, and annual precipitation series were derived from the daily series.

In this study, precipitation was defined as the total amount of daily precipitation in excess of 1 mm because precipitation <1 mm cannot be absorbed by soil and will rapidly evaporate. We selected 4 precipitation variables to investigate the spatial and temporal variation in precipitation in the study region. Daily precipitation ranges of 1–10, 10.1–25, 25.1–50, and >50 mm were denoted as P_1, P_2, P_3, and P_4, respectively. P_3 and P_4 represent heavy rain and rainstorms, which reflect heavy precipitation events. The total amount of P_1, P_2, P_3, and P_4 is denoted by TP_1, TP_2, TP_3, and TP_4, and the corresponding frequency (precipitation days) is denoted by PD_1, PD_2, PD_3, and PD_4. To assess the dry/wet conditions during the investigated period, 5 annual precipitation indices (annual precipitation, number of precipitation days, daily maximum precipitation, 5 d maximum precipitation, and precipitation intensity) were also selected, and the arithmetic means were calculated to represent the general wetness/dryness in this region. A similar application was executed in the Zhujiang River basin, and the detailed calculation of the integrated indicator is available in that study (Gemmer et al. 2011).

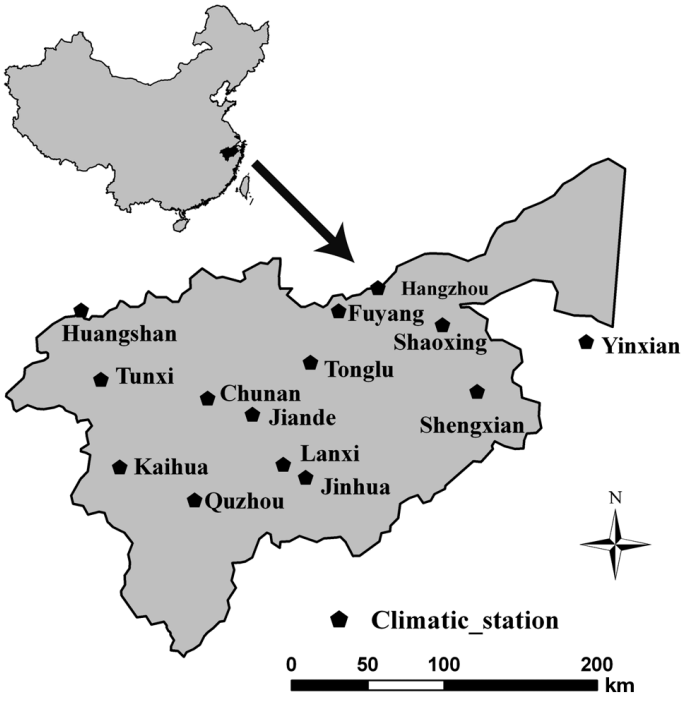

Fig. 1. Location of study region and climatic stations in the Qiantang River basin, eastern China

2.2. Trend analysis

Because precipitation data are always non-normally distributed, parametric statistical tests for trend analysis are not applicable. We therefore used an extensively applied non-parametric method, the Mann-Kendall (MK) method, which can be run without assuming any particular distribution (Mann 1945, Kendall 1975). The null hypothesis of this statistical test is that no trend is observed for the tested variable, and the significance level was set to 0.05. To estimate the magnitude of the trend in these precipitation indices, the method of Sen (1968) was used. Detailed information is available in Hu et al. (2012).

2.3. Empirical orthogonal functions

Empirical orthogonal functions (EOF) analysis is a technique to decompose a data set in terms of orthogonal basis functions, which are determined from the original data (North 1984). The objective of an EOF analysis is to decompose the dataset to identify some orthogonal spatial patterns (EOFs) and corresponding time series (principal components, PCs), which is similar to a principal components analysis. Since the EOF analysis produces p pairs of EOF/PC, the number of leading pairs must be determined. The total fraction of variance, which is explained by eigenvalues, should exceed 80%; the North criterion (North et al. 1982) was employed in this study. Normalized summer precipitation was used for the EOF analysis in this study. Detailed information about EOF analysis is available in Wu et al. (2012).

3. RESULTS AND DISCUSSION

3.1. Statistical behaviors of annual precipitation with different magnitudes

3.1.1. Annual precipitation with different magnitudes and their corresponding trends

The long-term annual average precipitation in this region is ~1600 mm, with spatial variation, declining from west to east (Fig. 2e). TP_2 (31.9 ± 2.7% SD) exhibits the largest contribution to the TP, followed by TP_3 (27.7 ± 1.0%), TP_1 (21.1 ± 2.4%), and TP_4 (19.3 ± 4.9%). Fig. 2 displays the spatial distribution of long-term averages of precipitation with different magnitudes. No significant spatial distribution characteristics for both TP_1 and TP_2, which represent light to moderate precipitation, were observed. Heavy precipitation events, including TP_3 and TP_4, declined from west to east, which indicates a spatial distribution similar to that of TP (Fig. 2e). The similar distribution of total (TP) and heavy precipitation (TP_3 and TP_4) indicates a linkage between them. High-elevation areas are primarily located in the western part of the study region, especially the northwest, and this geographical variation significantly affects the annual precipitation distribution in this region.

Although annual precipitation revealed no significant trends in terms of the regional average, it did show some spatial distribution characteristics from the aspect of individual stations (Fig. 3e). All stations showed an increasing trend in annual precipitation, with the exception of Huangshan

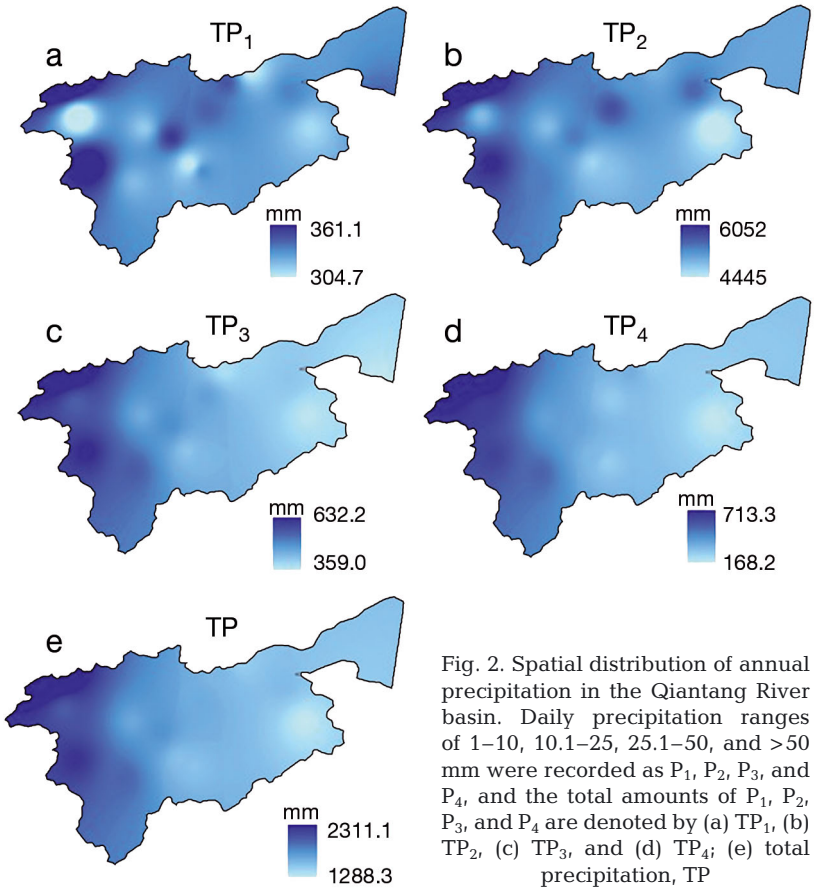

Fig. 2. Spatial distribution of annual precipitation in the Qiantang River basin. Daily precipitation ranges of 1–10, 10.1–25, 25.1–50, and >50 mm were recorded as P_1, P_2, P_3, and P_4, and the total amounts of P_1, P_2, P_3, and P_4 are denoted by (a) TP_1, (b) TP_2, (c) TP_3, and (d) TP_4; (e) total precipitation, TP

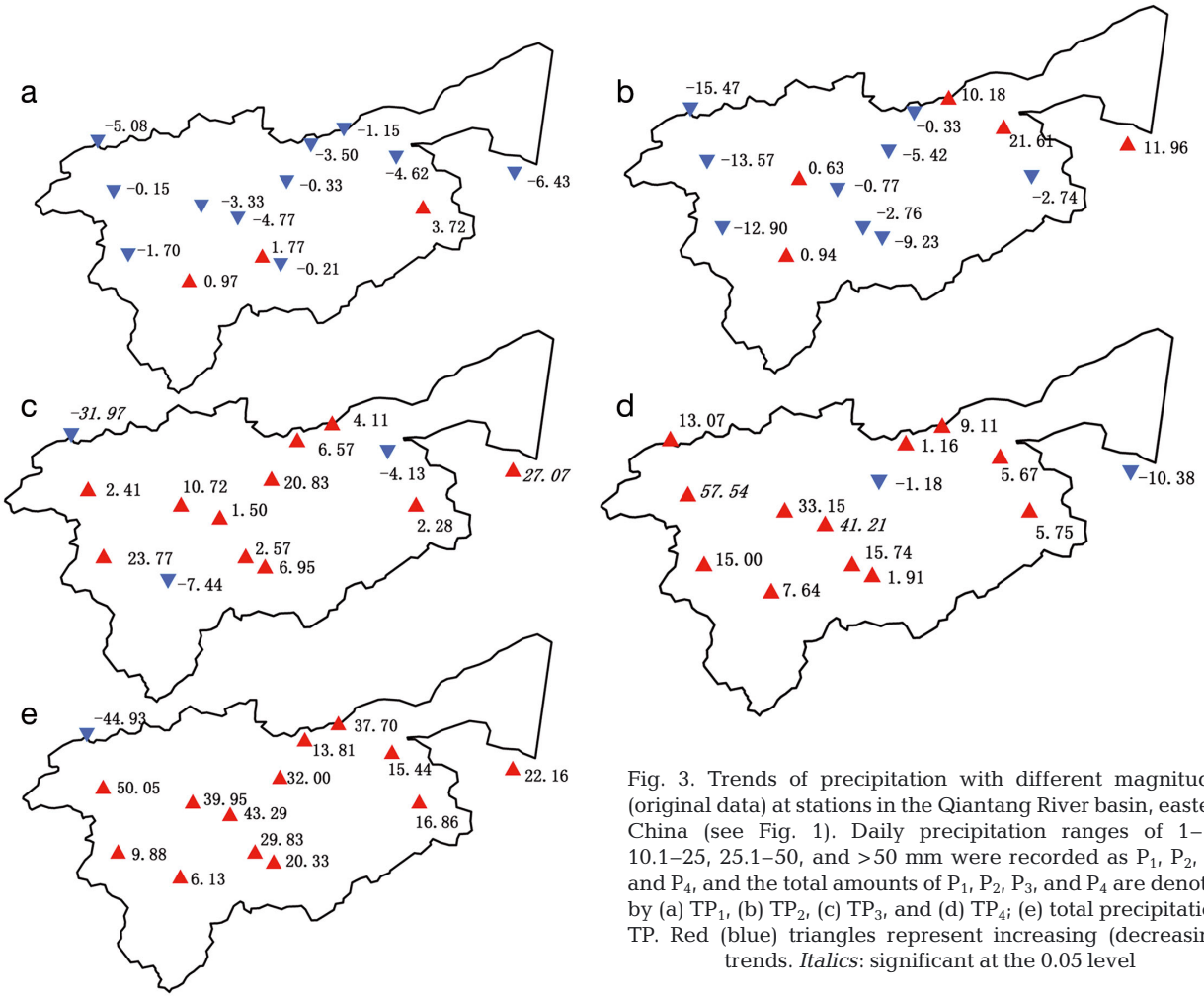

Fig. 3. Trends of precipitation with different magnitudes (original data) at stations in the Qiantang River basin, eastern China (see Fig. 1). Daily precipitation ranges of 1–10, 10.1–25, 25.1–50, and >50 mm were recorded as P_1, P_2, P_3, and P_4, and the total amounts of P_1, P_2, P_3, and P_4 are denoted by (a) TP_1, (b) TP_2, (c) TP_3, and (d) TP_4; (e) total precipitation, TP. Red (blue) triangles represent increasing (decreasing) trends. *Italics*: significant at the 0.05 level

station, which recorded a decrease (−44.93 mm decade^{-1}). The greatest increase was detected at Tunxi station, with a magnitude of 50.05 mm decade^{-1}. The increase is greater in the north of the region. The annual precipitation days (PDs) revealed a decreasing trend throughout the region, and half of the stations showed significant reductions (Table 1). The opposite trend in TP and PDs reflects the occurrence of more intense precipitation events in recent decades.

To identify detailed changes in precipitation, precipitation of different magnitudes was also examined at these stations (Fig. 3a–d). The results revealed that the trend in spatial distribution patterns varied with magnitude. More stations in the study region showed a decreasing trend in TP_1 and TP_2, whereas an increasing trend was predominant in TP_3 and TP_4. The largest decrease in TP_1 was identified at the coastal station Yinxian, whereas the largest increase occurred at Shengxian station. The north–south inverse phase pattern was denoted by the trend of TP_1, in

Table 1. Mann-Kendall test of frequencies of daily precipitation ranges of 1–10, 10.1–25, 25.1–50, and >50 mm (PD_1, PD_2, PD_3, and PD_4) in the Qiantang River basin, eastern China. **Bold**: significant at the 0.05 level. PDs: precipitation days

Station	PD_1	PD_2	PD_3	PD_4	PDs
Hangzhou	**−8.57**	0.37	0	0	−2.14
Quzhou	−2.41	0	0	0	−2.4
Tunxi	**−7.73**	−0.8	0	**0.67**	−2.14
Shengxian	0	−0.32	0	0	1.14
Yinxian	**−13.81**	0.37	**0.87**	0	**−2.86**
Chunan	**−3.1**	0	0.31	0.33	−2.35
Huangshan	**−3.33**	−0.65	−0.81	0	**−3.33**
Fuyang	**−11.43**	0	0	0	**−10.5**
Jiande	**−4.14**	0	0	**0.57**	**−3.2**
Tonglu	**−4.38**	0	0.43	0	**−3.53**
Lanxi	−1.9	0	0	0	−1.79
Jinhua	−2.95	0	0	0	0
Kaihua	**−16.33**	−0.57	0.56	0	**−15.64**
Shaoxing	**−4.29**	1.07	0	0	−3

which the southern part of the region primarily showed an increasing trend. The largest decrease in TP_2 was identified at Huangshan station, and Shaoxing had the largest increase in the region. Disregarding the trend direction in TP_2, the trend magnitude of the stations in the central region was much smaller. The largest significant increase in TP_3 of 27.07 mm decade^{-1} was recorded at Yinxian station. The largest decrease in TP_3 (–31.97 mm decade^{-1}) was identified at Huangshan station. Neither the trend nor the magnitude of TP_3 showed any distinct spatial characteristics. The largest increase in TP_4 of 57.54 mm decade^{-1} was detected at Tunxi station. The magnitude of the trend in TP_4 displays a decreasing spatial pattern from west to east, in which the greater increase occurred in the west. The trends of corresponding frequencies are summarized in Table 1. The frequencies of P_1 are identified with significant decreases in most stations. However, the majority of the stations in the study region showed no trend for the frequencies of P_2, P_3, and P_4.

The variation in the integrated indicator for wet/dry conditions is shown in Fig. 4. The year 1978 was identified to be the severest dry year, whereas 1973, 1994, and 1997 were the wettest years in the investigated period. The integrated precipitation indicator displayed striking characteristics of inter-decadal variation. This region experienced relative dryness during the 1960s and 1980s, whereas it received sufficient precipitation during the 1990s. The 1970s were considered a decade with an equal frequency of variation between dry and wet conditions. The wet condition in the 1990s was consistent with the result of the entire country of China, which was based on area-averaged annual anomalies (Zhai et al. 2005). The distinct increase after the late 1980s was very likely caused by global warming, which is primarily caused by excessive greenhouse gas emissions (Wentz et al. 2007). In the late 1980s, an economic boom occurred in Zhejiang Province, which was primarily dependent on industrial development. This boom prompted a sudden increase in greenhouse emissions and resulted in increased precipitation in this region. The integrated precipitation indicator showed a sharp decrease after 2002, which was also identified in the Yangtze River region (Zhu et al. 2011). Due to the incompleteness of the precipitation data in the 2000s, the decrease cannot be considered to be characteristic of the precipitation in the 2000s and requires additional investigation for the entire 2000s. The change in dry/wet conditions in the past 2 decades, as indicated by the integrated precipitation index, is similar to the change in dry/wet conditions in the neighboring Hunan Province, as indicated in an investigation of the annual standardized precipitation index (Du et al. 2013).

Precipitation is controlled not only by the atmospheric water vapor content, but also by vertical velocity. The change in atmospheric moisture, as identified in observations via model fingerprints, was caused by external anthropogenic forcing (Santer et al. 2007). Global warming, which is caused by excessive emissions of greenhouse gases, contributes to increased precipitation in the Northern Hemisphere (Min et al. 2011) by increasing atmospheric water vapor with increasing temperature and the change of vertical motion, as expected by the Clausius-Clapeyron relation (Chen et al. 2011). However, a previous study showed a decreased atmospheric water content in the Yangtze-Huaihe region after the 1960s (Cao & Ge 2004). Although a decreasing trend was also recorded in annual average humidity in this region, the correlation between daily precipitation and daily humidity revealed a significant positive correlation. Regional factors are also important to the precipitation in this region. Aerosols, which are primarily determined by regional emission sources, such as local industry and traffic, will

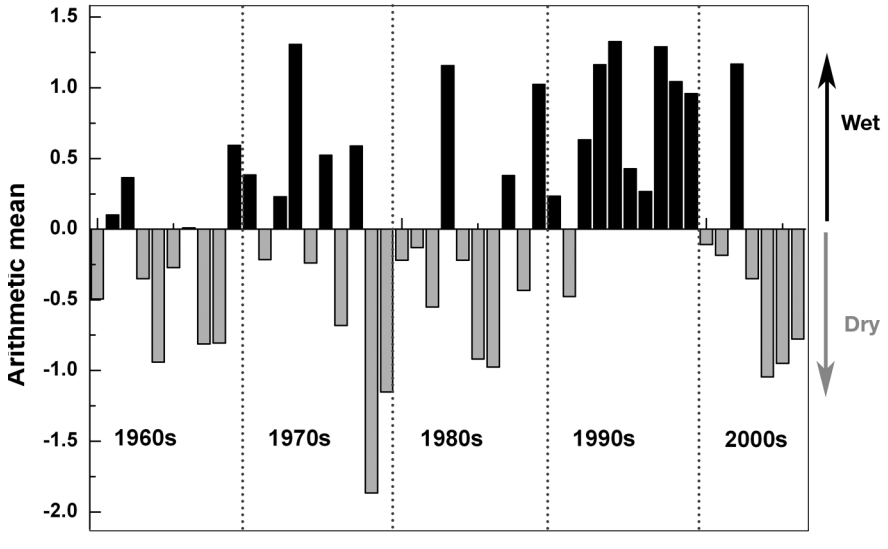

Fig. 4. Arithmetic mean of 5 standardized precipitation indices (annual precipitation, number of precipitation days, maximum daily precipitation, maximum 5 d precipitation, precipitation intensity) for the period of 1960–2006 in the Qiantang River basin, eastern China

significantly affect precipitation at a regional scale, because they cannot mix as well as greenhouse gases. Due to the industrial structure of dispersed individual factories, which heavily depend on the combustions of fossil fuels, these workshops generate a large amount of aerosols in this region. Aerosols can change the distribution, form, and frequency of precipitation by acting as cloud condensation nuclei (Fan et al. 2012). Total precipitation and extreme precipitation events may increase due to the effect of aerosols on cloud seeding (Rosenfeld et al. 2008). Modeling research has shown the direct and indirect impact of aerosols on seasonal precipitation (Huang et al. 2007). The increase in aerosols has already caused frequent haze and incited public concern in eastern China (Shi et al. 2010); aerosols also play a role in precipitation change.

3.1.2. Annual extreme precipitation

Due to the vital role of extreme precipitation in meteorological disasters, such as floods and droughts, the extreme precipitation events in the study region should be analyzed to inform decision making related to water resource management and meteorological disaster warning. The daily extreme precipitation indices showed similar behavior during the study period. We selected the total amount and the number of days of daily precipitation that exceeded the 95th percentile (P95) during the study period (TP95 and PD95) to represent the detailed variation in extreme precipitation in the study region (Fig. 5). The year 1983 had the most extreme precipitation events, whereas 1978 had the fewest extreme precipitation events. The comparison (1-way ANOVA) demonstrated a significant difference in intensity and frequency before and after the mid-1980s (i.e. much greater after the mid-1980s). The evolution of extreme precipitation events (TP95 and PD95) can be divided into 2 stages in the study period, according to the variation trend. The trend analysis showed a general increasing trend before the late 1980s and an opposite trend after the late 1980s.

In addition to a sudden heavy shower, consecutive extreme precipitation events can also cause droughts/floods. In this study, we selected annual consecutive dry/wet days (CDD/CWD) and maximum consecutive 5 d precipitation (RX5D) to show the duration of consecutive precipitation events (including dry/wet conditions). Because these indices are weakly correlated with each other, they can provide comprehensive information about extreme dry/wet climates. As shown in Fig. 6, the changes (before/after 1990) in these 3 indices are consistent with each other and indicate more extreme precipitation events after 1990. We identified 10 out of 30 years with more than 30 CDDs prior to 1990; the severest dry year occurred in 1974, with 44 CDDs. However, only 3 out of 16 years had >30 CDDs after 1990. CWDs did not significantly change before/after 1990; the maximum value of 15 was recorded in 1992. From the perspective of individual stations, 9 of 14 stations showed an insignificant decrease in CDDs and 11 of 14 stations displayed an insignificant increase in CWDs. The regional RX5D displayed an insignificant increase over the entire investigated period. The regional average of RX5D was 164.3 mm prior to 1990; 198.7 mm was subsequently attained. The comparison showed a statistically significant difference before/after 1990. Four stations recorded a decreasing trend in RX5D, whereas the remaining 10 stations identified an increasing trend; of these, 4 showed a significant increase. Although the trends in these indices were not statistically significant for most stations, the significant difference before/after 1990 in CDD and RX5D implies less continuous dry weather and more heavy precipitation events in the recent 2 decades.

IPCC projected an increase in heavy precipitation events by multiple models (IPCC 2014), which was

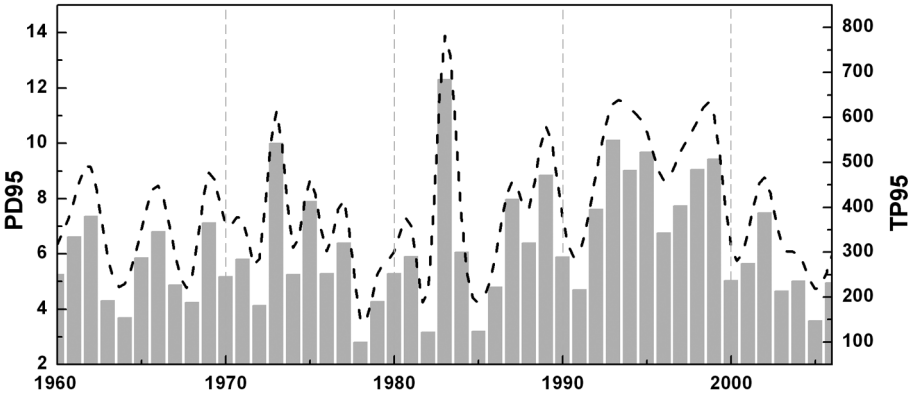

Fig. 5. Annual total precipitation and number of days with precipitation that exceeded the 95th percentile (TP95 and PD95) in the Qiantang River basin, eastern China. Bars represent PD95, and the dotted line represents TP95

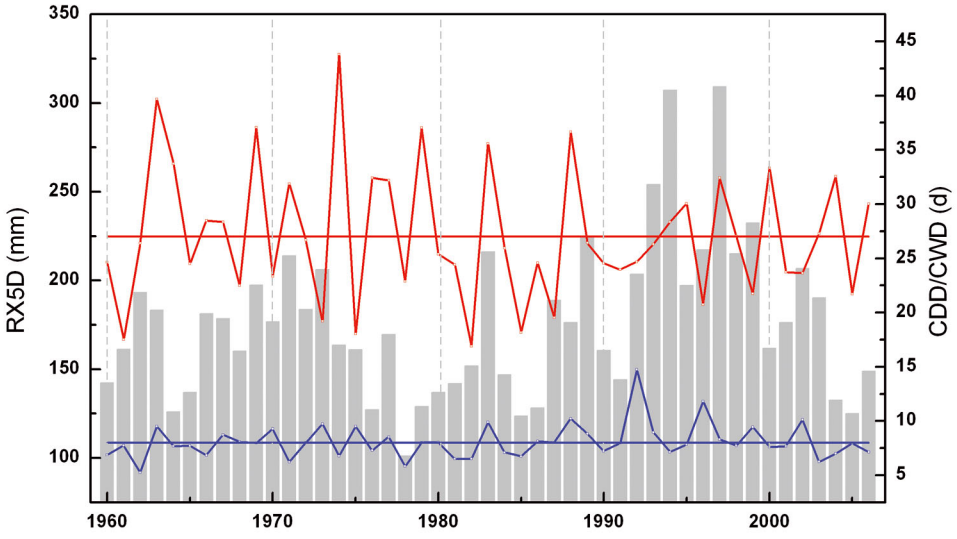

Fig. 6. Time series of extreme precipitation events in the Qiantang River basin, eastern China. The bars represent maximum consecutive 5 d precipitation (RX5D), the red (blue) curve represents consecutive dry (wet) days (CDD [CWD]), and the red (blue) straight line represents the long-term average of CDD (CWD)

consistent with China's National Assessment Report on Climate Change (CMA 2014). An increase in extreme precipitation was also identified in the study region. An increase in extreme precipitation is related to an increase in atmospheric water content, which is a thermodynamic change in precipitation (Emori & Brown 2005). However, more than half of the stations recorded a significant decrease in annual humidity in this region, which may be attributed to the southward transportation of moisture (Zhu et al. 2011). A previous study indicated that precipitation extremes had a stronger relationship with near-surface water vapor concentrations than with the total atmospheric water content (O'Gorman & Schneider 2009). Agriculture in our study region is widely practiced with dispersed farming, with an irrigation pattern of flood-irrigation supplemented by furrow-irrigation, which leads to a longer period of irrigation than that for intensive agriculture. An extensive duration of irrigation has a direct influence on atmospheric water vapor abundance near the surface (Boucher et al. 2004), which is likely attributed to an increase in the evapotranspiration and precipitable water (DeAngelis et al. 2010). A significant water-covered area, including coastal areas and shallows in this region, was reclaimed for arable and residential land over recent decades to satisfy the demand of urban construction (Yao et al. 2007). The ability to adjust the floods in the study region can be affected by the reduction in the water-covered area and the increase in urbanization (Miller et al. 2014). Both the irrigation pattern and the land cover change will affect the energy flux and surface water vapor, as well as the extreme precipitation events in this region.

3.2. Spatio-temporal evolution of summer precipitation

3.2.1. Characteristics of precipitation in summer

Summer precipitation substantially contributes to the annual total precipitation and is vital to the water resources in this region. Thus, we made a detailed analysis of the summer precipitation in this study. The long-term average spatial distribution of summer precipitation is similar to the spatial distribution of annual precipitation, which decreases from west to east and for which the highest value was identified at the mountainous Huangshan station.

The annual summer precipitation anomaly from 1960–2006 for the regional average is shown in Fig. 7. This region displayed a significant increase of 35.53 mm decade^{-1} during the study period. The inter-decadal variation in summer precipitation is similar to the inter-decadal variation in annual precipitation. This finding is primarily attributed to the large contribution of summer precipitation to the annual total precipitation (35.3 ± 6.5%). Prior to the mid-1970s, the study region was primarily dominated by consecutive dry conditions, with the exception of 1969. The most striking characteristic of summer precipitation in the study region is the apparent transition to consecutive wet periods in approximately 1992, which was also reported by Qian & Qin (2008). This is mainly attributed to an increase in the lower-level convergence, the mid-tropospheric ascent, and the upper-level divergence in southern China (Wu et al. 2010). After 2002, however, the situation changed; the study region experienced consecutive dry summers.

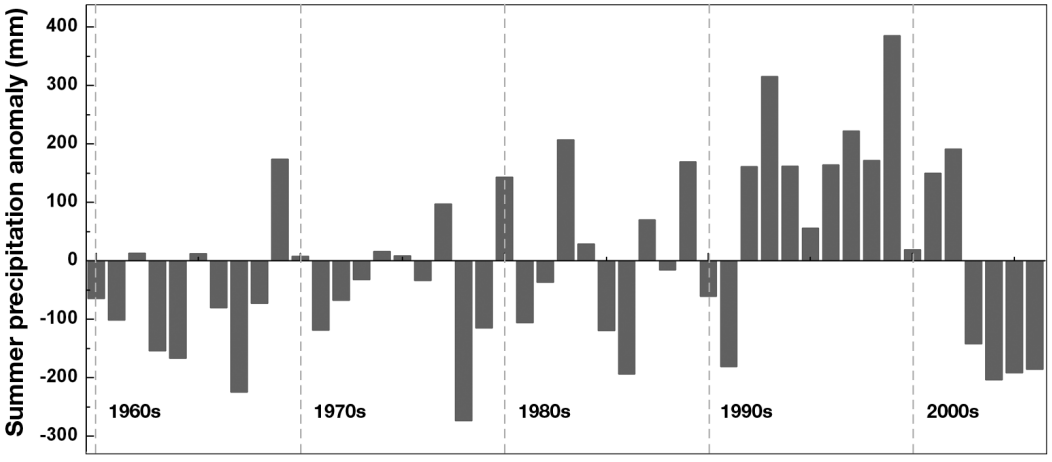

Fig. 7. Time series of summer precipitation anomalies in the Qiantang River basin, eastern China

The study region is located along the route of monsoon migration, which is sensitive to the Asian summer monsoon. A previous study verified the weakening of the Asian summer monsoon (Ding et al. 2008), which substantially impacts the summer precipitation in this region. Yuan et al. (2010) analyzed the movement of the monsoon rain belt in summer and discovered that mid-June and the period from mid-July to mid-August comprised the 2 main rainy seasons during summer in eastern China (including the study region), which followed the East Asian summer monsoon circulation and the formation of an active-break-revival pattern. In addition, summer precipitation in east China is highly dependent on El Niño events and corresponding atmospheric motion, which impacts the climate in south China and produces more precipitation (Wu & Hu 2003). In this paper, most stations recorded a positive summer precipitation anomaly in the El Niño decaying summer, which was confirmed by the positive correlation between summer precipitation and prior El Niño events (data not shown). The precipitation variation during El Niño events is primarily attributed to the evolution of the Western North Pacific anti-cyclone and the westward shift of the ridge of a sub-tropical high during the El Niño decaying phase (Feng et al. 2011).

3.2.2. EOF analysis in summer

The EOF analysis was applied to summer precipitation, and pairs of EOFs/PCs are shown in Fig. 8. According to the variation captured and the significance of the North test, the first 3 pairs were selected, which primarily reflected the structure of the precipitation variation in the study region. The variance proportion of EOF1 reached 66.76%, followed by EOF2 and EOF3, which contributed 10.76 and 7.24%, respectively. The cumulative variance proportion of the first 3 EOFs is >80% of the total variance. The variance proportion of EOF1 in summer is considerably less than the variance proportion of EOF1 in winter (91.31%). This is attributed to similar large-scale characteristics of the winter precipitation and complicated local redistribution of summer precipitation, which requires additional modes to capture the precipitation variation in summer. The eigenvectors in EOF1 in summer revealed a positive phase consistency, which indicated that the entire region experienced the same variation in summer precipitation. The result was supported by the consistent increase in summer precipitation for all stations. The eigenvector values of EOF1 in summer displayed a distinct spatial pattern, which showed a decreasing trend from west to east. This spatial distribution is similar to the spatial distribution of the long-term average precipitation (Fig. 2e). Although the second and third modes of summer precipitation captured significantly less variance compared to EOF1, they displayed completely different spatial distribution patterns. There are both positive and negative values of eigenvectors in EOF2 and EOF3. EOF2 is donated by a north–south inverse pattern, whereas EOF3 is identified with a west–east inverse pattern. The north is marked with positive values in EOF2, whereas the west is represented by positive values in EOF3 in summer.

The corresponding PCs are capable of representing the temporal variation in summer precipitation. We provide detailed information about PC1 and a brief introduction to PC2 and PC3 because the first mode captured large features of the total variance. The MK trend analysis showed that the PC1 of summer precipitation displayed a statistically significant

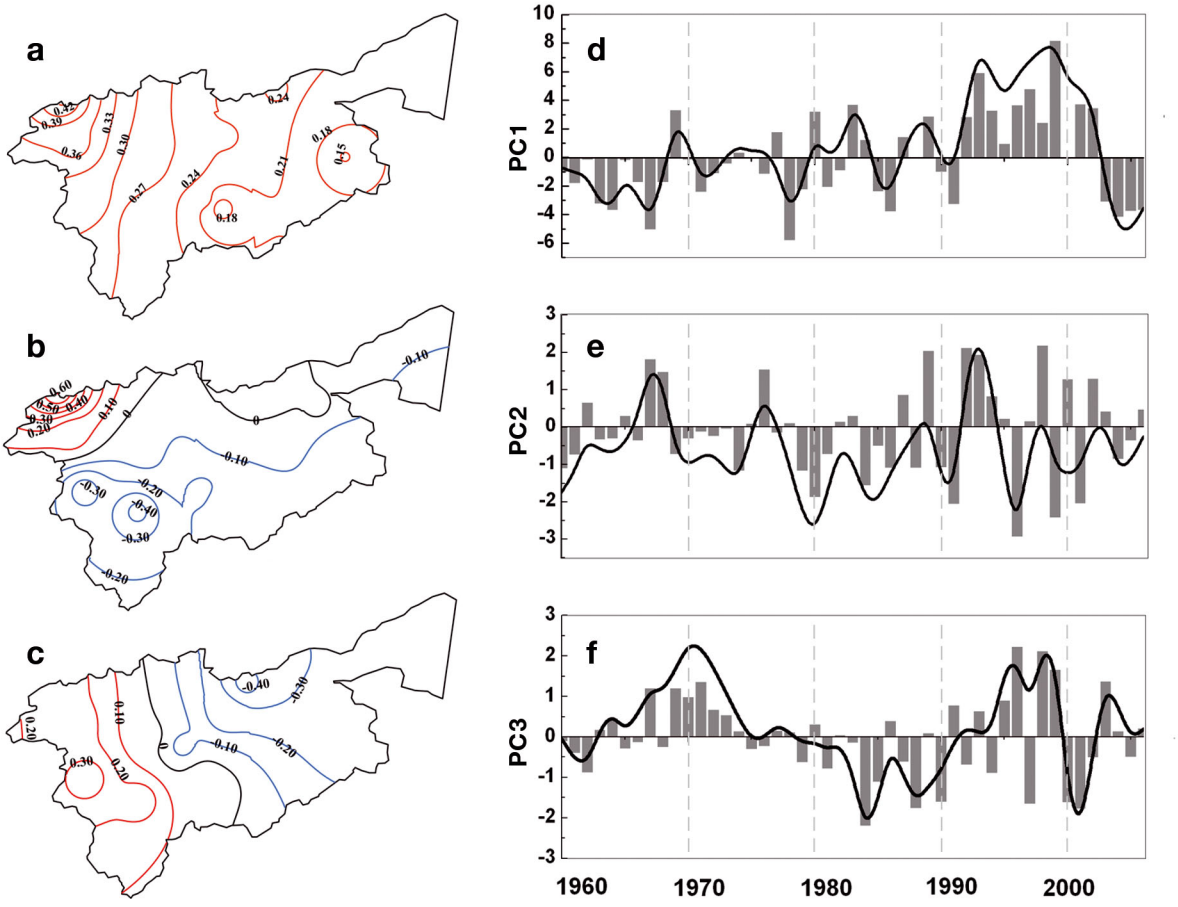

Fig. 8. (a–c) Empirical orthogonal functions (EOFs) and (d–f) corresponding time series (principal components, PCs) of summer precipitation in the Qiantang River basin, eastern China. The black lines in the EOFs represent a 0 value, and the red (blue) lines represent positive (negative) values. The solid curves represent a 3 yr moving average with binomial coefficients in PCs

increase, with a Z value of 2.04. The increasing trend in PC1 of summer precipitation is consistent with the increased summer precipitation in the study region. The similarity is apparent in the change of PC1 and the summer precipitation (Fig. 7). This result confirmed that the first EOF/PC pair captured the majority of the variation in the summer precipitation during the study period on a spatial and temporal scale. The study region underwent 3 main periods for PC1 during the study period, namely a dry stage (1960–1975), a fluctuating stage (1976–1991), and a wet stage (1992–2002), which indicated a transition from dry periods to wet periods. The wet conditions changed after 2002, which was also identified in the annual precipitation. PC2 differs from PC1, which indicated more fluctuation in the entire period, and PC3 displayed a wet–dry fluctuating pattern.

The EOF analysis showed spatial and temporal variation in summer precipitation. The results revealed spatial variations among the selected modes. Located in eastern China, this area is highly sensitive to the monsoon climate and is characterized by convective activity. In addition, the large scale of moisture transportation and local vertical winds contribute to the distribution of summer precipitation. PCs, especially the important PC1, primarily reflect large-scale circulation, such as the Pacific decadal oscillation, the Western Pacific Subtropical High (which showed a positive correlation with summer precipitation in this study), and the East Asian summer monsoon (Zhu et al. 2011). The change patterns of EOFs/PCs require additional investigations to understand their detailed physical mechanisms.

4. CONCLUSIONS

Generally, precipitation in the study region showed an increasing tendency from 1960–2006. TP_3 and TP_4 significantly contributed to the total precipitation and

displayed a spatial distribution similar to annual precipitation. Light precipitation (TP_1 and TP_2) was dominated by a decreasing trend at most stations, whereas TP_3 and TP_4 showed an increasing tendency at most stations. The integrated indicator of annual precipitation displayed a striking inter-decadal variation, with a transition from dry conditions to wet conditions. Extreme precipitation events (P95) evolved toward more intense and frequent events, which increased the potential for future flooding. The evolution of extreme precipitation can be divided into 2 stages: a general increase prior to the late 1980s and a general decrease after the late 1980s. The analysis of consecutive dry/wet conditions revealed that the study region experienced a transition of CDDs to CWDs.

Summer precipitation makes a significant contribution to the annual total precipitation, which demonstrates a spatial distribution and temporal variation similar to that of annual precipitation. The EOF analysis showed that the first 3 modes captured the majority of the variance in summer precipitation. The eigenvector values of EOF1 in summer were all positive, which indicates the same variation throughout the region during the study period. The second and third modes showed distinct spatial differences, with a north–south inverse pattern in EOF2 and a west–east inverse pattern in EOF3. The representative temporal variation in PC1 showed a general increase, which represented the primary change in the summer precipitation.

Climate change is very likely caused by excessive emissions of greenhouse gases in the 20th century, which have caused increased temperatures and a redistribution of precipitation on a global scale. The study region is located in the East Asian monsoon area, which is sensitive to climate change. Regional factors, including aerosols, irrigation patterns, and reclamation, affect regional precipitation, especially extreme precipitation events. This study provides detailed information about the change in precipitation in previous decades and will aid in forecasting future precipitation and meteorological disasters. To comprehensively understand changes in precipitation and their physical mechanisms, additional investigation is necessary to distinguish the primary and secondary factors that affect precipitation in this region.

Acknowledgements. This research was sponsored by the National Natural Science Foundation project of China (41171258, 41271048), the Zhejiang Provincial Natural Science Foundation of China (LR13D010001), and the Science and Technology Project of Zhejiang Province (2011C13010). We thank the China Meteorological Administration and Zhejiang Meteorological Administration for providing the data for this study. We also appreciate the laboratory group for assistance with data analysis.

LITERATURE CITED

Alexandersson H, Moberg A (1997) Homogenization of Swedish temperature data. I. Homogeneity test for linear trends. Int J Climatol 17:25–34

Boucher O, Myhre G, Myhre A (2004) Direct human influence of irrigation on atmospheric water vapour and climate. Clim Dyn 22:597–603

Bouwer LM (2011) Have disaster losses increased due to anthropogenic climate change? Bull Am Meteorol Soc 92:39–46

Buishand TA (1982) Some methods for testing the homogeneity of rainfall records. J Hydrol (Amst) 58:11–27

Bukovsky MS, Karoly DJ (2011) A regional modeling study of climate change impacts on warm-season precipitation in the central United States. J Clim 24:1985–2002

Cao LQ, Ge ZX (2004) Characteristics of average water content in the atmosphere in Yangtze-Huaihe region and its variation. J Hehai Univ 32:636–639 (in Chinese)

Chaplot V (2007) Water and soil resources response to rising levels of atmospheric CO_2 concentration and to changes in precipitation and air temperature. J Hydrol (Amst) 337:159–171

Chen L, Frauenfeld OW (2014) A comprehensive evaluation of precipitation simulation over China based on CMIP5 multimodel ensemble projections. J Geophys Res Atmos 119:5767–5786

Chen G, Ming Y, Singer ND, Lu J (2011) Testing the Clausius-Clapeyron constraint on the aerosol-induced changes in mean and extreme precipitation. Geophys Res Lett 38:L04807, doi:10.1029/2010GL046435

Chernoff H, Zacks S (1964) Estimating the current mean of a normal distribution which is subjected to changes in time. Ann Math Stat 35:999–1018

Chou C, Chiang JC, Lan CW, Chung CH, Liao YC, Lee CJ (2013) Increase in the range between wet and dry season precipitation. Nat Geosci 6:263–267

CMA (China Meteorological Administration, Ministry of Science and Technology) (2014) China's national assessment report on climate change (III). Science Press, Beijing (in Chinese)

Dai ZH, Zhou CS, Tao CH, He PD (1998) Records of Qiantang River. Fangzhi Press, Beijing (in Chinese)

DeAngelis A, Dominguez F, Fan Y, Robock A, Kustu MD, Robinson D (2010) Evidence of enhanced precipitation due to irrigation over the Great Plains of the United States. J Geophys Res 115:D15115, doi:10.1029/2010JD013892

Ding YH, Wang ZY, Sun Y (2008) Inter-decadal variation of the summer precipitation in East China and its association with decreasing Asian summer monsoon. I. Observed evidences. Int J Climatol 28:1139–1161

Dinpashoh D, Fakheri-Fard A, Moghaddam M, Jahanbakhsh S, Mirnia M (2004) Selection of variables for the purpose of regionalization of Iran's precipitation climate using multivariate methods. J Hydrol (Amst) 297: 109–123

Du J, Fang J, Xu W, Shi PJ (2013) Analysis of dry/wet conditions using the standardized precipitation index and its

potential usefulness for drought/flood monitoring in Hunan Province, China. Stochast Environ Resident Risk Assess 27:377–387

Emori S, Brown SJ (2005) Dynamic and thermodynamic changes in mean and extreme precipitation under changed climate. Geophys Res Lett 32:L17706, doi:10.1029/2005GL023272

Fan JW, Leung LR, Li ZQ, Morrison H and others (2012) Aerosol impacts on clouds and precipitation in eastern China: results from bin and bulk microphysics. J Geophys Res Atmos 117:D00K36, doi:10.1029/2011JD016537

Feng J, Chen W, Tam CY, Zhou W (2011) Different impacts of El Niño and El Niño Modoki on China rainfall in the decaying phases. Int J Climatol 31:2091–2101

Gardner LA (1969) On detecting changes in the mean of normal variates. Ann Math Stat 40:116–126

Gemmer M, Fischer T, Jiang T, Su BD, Liu LL (2011) Trends in precipitation extremes in the Zhujiag River basin, south China. J Clim 24:750–761

Hu ZZ (1997) Interdecadal variability of summer climate over East Asia and its association with 500 hPa height and global sea surface temperature. J Geophys Res 102: 19403–19412

Hu YR, Maskey S, Uhlenbrook S (2012) Trends in temperature and rainfall extremes in the Yellow River source region, China. Clim Change 110:403–429

Huang Y, Chameides WL, Dickinson RE (2007) Direct and indirect effects of anthropogenic aerosols on regional precipitation over east Asia. J Geophys Res 112:D03212, doi:10.1029/2006JD007114

IPCC (Intergovenmental Panel on Climate Change) (2013) Climate change 2013: the physical science basis. Contribution of Working Group I to the fifth assessment report. Cambridge University Press, Cambridge

IPCC (2014) Climate Change 2014: synthesis report. Cambridge University Press, Cambridge

Kendall MG (1975) Rank correlation measures. Charles Griffin, London

Kunkel KE, Easterling DR, Redmond K, Hubbard K (2003) Temporal variations of extreme precipitation events in the United States: 1895–2000. Geophys Res Lett 30:1900, doi:10.1029/2003GL018052

Mann HB (1945) Non-parametric tests against trend. Econometrica 13:245–259

Miller JD, Kim H, Kjeldsen TR, Packman J, Grebby S, Dearden R (2014) Assessing the impact of urbanization on storm runoff in a peri-urban catchment using historical change in impervious cover. J Hydrol (Amst) 515:59–70

Min SK, Zhang XB, Zwiers FW, Hegerl GC (2011) Human contribution to more-intense precipitation extremes. Nature 470:378–381

North GR (1984) Empirical orthogonal functions and normal modes. J Atmos Sci 41:879–887

North GR, Bell TL, Cahalan RF, Moeng FJ (1982) Sampling errors in the estimation of empirical orthogonal functions. Mon Weather Rev 110:699–706

O'Gorman PA, Schneider T (2009) The physical basis for increases in precipitation extremes in simulations of 21st-century climate change. Proc Natl Acad Sci USA 106:14773–14777

Pettitt AN (1979) A non-parametric approach to the change-point problem. Appl Stat 28:126–135

Piao SL, Ciais P, Huang Y, Shen ZH and others (2010) The impacts of climate change on water resources and agriculture in China. Nature 467:43–51

Portmann RW, Solomon S, Hegerl GC (2009) Spatial and seasonal patterns in climate change, temperatures, and precipitation across the United States. Proc Natl Acad Sci USA 106:7324–7329

Qian WH, Qin A (2008) Precipitation division and climate shift in China from 1960 to 2000. Theor Appl Climatol 93: 1–17

Rosenfeld D, Lohmann U, Raga GB, O'Dowd CD and others (2008) Flood or drought: How do aerosols affect precipitation? Science 321:1309–1313

Santer BD, Mears C, Wentz FJ, Taylor KE and others (2007) Identification of human-induced changes in atmospheric moisture content. Proc Natl Acad Sci USA 104: 15248–15253

Sen PK (1968) Estimates of the regression coefficient based on Kendall's tau. J Am Stat Assoc 63:1379–1389

Shi J, Cui LL, He QS, Sun L (2010) The changes and causes of fog and haze days in eastern China. Acta Geogr Sin 65:533–541(in Chinese)

Štěpánek P (2008) AnClim-software. Available at www.climahom.eu/software-solution/anclim

Tian Y, Xu YP, Booij MJ, Lin SJ, Zhang QQ, Lou ZH (2012) Detection of trends in precipitation extremes in Zhejiang, east China. Theor Appl Climatol 107:201–210

Twardosz R, Łupikasza E, Niedźwiedź T, Walanus A (2012) Long-term variability of occurrence of precipitation forms in winter in Kraków, Poland. Clim Change 113: 623–638

Wang HJ (2001) The weakening of the Asian monsoon circulation after the end of 1970s. Adv Atmos Sci 18: 376–386

Wentz FJ, Ricciardulli L, Hilburn K, Mears C (2007) How much more rain will global warming bring? Science 317: 233–235

Wu FF, Wang X, Cai YP, Yang ZF, Li CH (2012) Spatiotemporal analysis of temperature-variation patterns under climate change in the upper reach of Mekong River basin. Sci Total Environ 427-428:208–218

Wu RG, Hu ZZ (2003) Evolution of ENSO-related rainfall anomalies in East Asia. J Clim 16:3742–3758

Wu RG, Wen ZP, Yang S, Li YQ (2010) An interdecadal change in southern China summer rainfall around 1992/93. J Clim 23:2389–2403

Wu ZT, Dijkstra P, Koch GW, Penuelas J, Hungate BA (2011) Responses of terrestrial ecosystems to temperature and precipitation change: a meta-analysis of experimental manipulation. Glob Change Biol 17:927–942

Xia F, Liu XM, Xu JM, Wang ZG, Huang JF, Brookes PC (2015) Trends in the daily and extreme temperatures in the Qiantang River basin, China. Int J Climatol 35:57–68

Xu YP, Zhang XJ, Tian Y (2012) Impact of climate change on 24 h design rainfall depth estimation in Qiantang River Basin, East China. Hydrol Process 26:4067–4077

Xu YP, Ma C, Pan SL, Zhu Q, Ran QH (2014) Evaluation of a multi-site weather generator in simulating precipitation in the Qiantang River Basin, East China. J Zhejiang Univ Sci A Appl Phys Eng 15:219–230

Yao W, Lou JY, Zhang LS, Zhang Y, Liu P, Wu JP (2007) Land use/land cover dynamic in Qiantang river watershed: 1985–2004. Bull Sci Technol 4:502–507 (in Chinese)

Ye JS, Li WH, Li LF, Zhang F (2013) 'North drying and south wetting' summer precipitation trend over China and its potential linkage with aerosol loading. Atmos Res 125-126:12–19

You QL, Kang SC, Aguilar E, Pepin N and others (2011)

Changes in daily climate extremes in China and their connection to the large scale atmospheric circulation during 1961-2003. Clim Dyn 36:2399–2417

Yu L, Li KR, Tao B (2012) Assessment on ecosystem vulnerability to extreme precipitation in the middle and lower Yangtze Valley. J Nat Resour 27:82–89 (in Chinese)

Yuan WH, Yu RC, Chen HM, Li J, Zhang MH (2010) Subseasonal characteristics of diurnal variation in summer monsoon rainfall over central eastern China. J Clim 23: 6684–6695

Zhai PM, Zhang XB, Wan H, Pan XH (2005) Trends in total precipitation and frequency of daily precipitation extremes over China. J Clim 18:1096–1108

Zhang Q, Xu CY, Chen XH, Zhang ZX (2011) Statistical behaviors of precipitation regimes in China and their links with atmospheric circulation 1960–2005. Int J Climatol 31:1665–1678

Zhu YL, Wang HJ, Zhou W, Ma JH (2011) Recent changes in the summer precipitation pattern in East China and the background circulation. Clim Dyn 36:1463–1473

Editorial responsibility: Eduardo Zorita, Geesthacht, Germany

Submitted: June 29, 2015; Accepted: November 27, 2015
Proofs received from author(s): March 9, 2016